The Analysis of Polystyrene and Polystyrene Aggregates into the Mega Dalton Mass Range by Cryodetection MALDI TOF MS

Alexander A. Aksenov and Mark E. Bier
Center for Molecular Analysis, Department of Chemistry, Carnegie Mellon University, Pittsburgh, Pennsylvania, USA

Mass spectra of atactic polystyrene were collected into the mega-dalton mass range with a matrix-assisted laser desorption ionization time of flight (MALDI TOF) mass spectrometer, which incorporates a cryodetector comprised of an array of 16 superconducting tunnel junctions (STJ). The STJ cryodetector, theoretically, has no loss in signal response at any mass compared with the reduced signal found at high mass when using a conventional secondary-ionization detector. Since ion detection at high m/z is one of the fundamental limitations of mass spectrometry (MS), the cryodetector was used to explore the high m/z limit of the MALDI TOF technique for the analysis of two polymer types. Mass spectra were collected for polystyrene at M_n 170, 400, 900, and 2000 kDa and polymethyl methacrylate (PMMA) at M_n 62.6 kDa and 153.7 kDa. For polystyrene, the data showed a trend toward increased aggregation and charge state with mass. The M_n 2 MDa polystyrene data revealed a peak at m/z 2.2 MegaTh and a charge state analysis revealed that these ions were primarily polystyrene aggregates with a mass of ~4 MDa. This aggregate assignment was possible because the cryodetector response allows for the determination of a charge state up to about four. The contribution of each charge state for a selected peak can be determined in this fashion. This analysis revealed the preferential formation of doubly charged even-numbered aggregates over odd-numbered aggregates for high molecular mass polystyrene. A potential mechanism for the aggregation process for doubly charged species is discussed.   (J Am Soc Mass Spectrom 2008, 19, 219–230) © 2008 American Society for Mass Spectrometry

Matrix-assisted laser desorption ionization (MALDI) was first introduced by Tanaka and coworkers [1, 2] and further developed and improved by Karas and Hillenkamp [3]. The MALDI technique was a major breakthrough in mass spectrometry and it has seen widespread use in chemical and biological research because it offers several key advantages. First, it is a relatively "soft" ionization technique that can produce intact low charge state molecular ions at low laser power. Second, like electrospray ionization (ESI), MALDI is suitable for the ionization of large nonvolatile molecules including synthetic polymers and biomacromolecules, which cannot be brought into the gas phase and ionized intact by most other more energetic introduction and ionization techniques. Third, the MALDI technique is more robust than ESI for samples that contain high concentrations of salts and buffers. And finally, because MALDI can be operated in a pulsed ionization mode, it can be conveniently coupled to a time-of-flight (TOF) mass spectrometer. The theory and applications of the MALDI method are reviewed elsewhere [4–6].

It is reasonable to assume that the MALDI technique may have an upper m/z limitation. For example, the laser desorption ionization (LDI) technique, is limited to ~1000 Da for intact biological molecules and a few kDa for synthetic polymers [7]. Compared with LDI, MALDI shows reduced fragmentation of macromolecules [8] and the mass range has been extended to several 100 kDa. This extension of the mass range is attributed to the abundant matrix, usually in a ratio of at least 1000:1 with the analyte that provides a gentle lift of the heavy ions into the gas phase. In addition, neutral species, which are present in the MALDI plume before dissipation, can provide collisional dampening to stabilize the ions formed before acceleration [9]. Despite the "unlimited mass range" of the TOF mass analyzer, the fundamental upper m/z limit of the MALDI process, whether for biological or synthetic polymers, has not been conclusively determined empirically. The high mass limitations of conventional detector systems cause a signal reduction at high m/z [10–12], so the upper mass limit of

the MALDI technique lies beyond the capabilities of conventional MALDI TOF MS systems. Even with an ideal detector, three reasons may explain the expected upper mass limit of the MALDI technique: (1) a less efficient molecule launch into the gas phase for macromolecules, (2) increased source fragmentation which is the result of the use of higher laser powers typically required to lift macromolecules into the gas phase, and (3) metastable decomposition, which can occur to a greater extent because of the higher laser power and longer flight times to the detector for massive ions [13]. Despite these limitations, Danis and Karr reported MALDI TOF MS of poly(methyl methacrylate) (PMMA) at a molecular weight of ~256 kDa [14]; Schriemer and Li have reported the detection of singly charged and multiply charged polystyrene for M_n 900 kDa and 1.5 MDa at 900 kTh for $[M + Ag]^{+1}$ and 750 kTh for $[M + 2Ag]^{+2}$, respectively [15], and Nelson et al. reported the detection of human monoclonal immunoglobulin M (IgM) at ~1 MDa with charge states of +2 to +6 [16]. In all of these experiments, the researchers used conventional, secondary emission based detectors, which inherently show a decreased signal with increased mass [13].

Advances have been made in detection technology to circumvent the problem of decreased sensitivity at high m/z. Post-acceleration detection using ion conversion dynodes shows superior performance at high m/z compared with using only microchannel plates (MCP) [17], but the signal response from a dynode is still ion velocity dependent. Faraday cup detectors have no signal decrease for high m/z, but pose other limitations, such as large response times [18] and no built-in signal amplification. Within the last 10 years, superconducting tunnel junction (STJ) cryodetectors have been coupled to TOF mass spectrometers [13, 19–22]. Twerenbold et al. have shown experimentally that STJ cryodetectors exhibit mass independent 100% detection efficiency [13]. Cryodetector technology has been employed to observe many different high m/z analytes with a different chemical nature. For example, the following analytes were all detected with a STJ cryodetector: polystyrene at 200 kDa and polystyrene aggregates up to 800 kDa [23], polyphenylene dendrimers up to 1 MDa [24], proteins and protein complexes such as anti-human influenza virus hemagglutinin/glutathione S-transferase containing an HA tag [AntiHA·GST-HA]$^+$ at 150–400 kDa [25], human immunoglobulin M (IgM) at ~1 MDa, and Von Willenbrand factor up to 1 MDa [26]. The principles of the operation of cryodetectors are discussed in detail elsewhere [22, 27].

Despite the above exceptional high mass results, the use of cryodetection in mass spectrometry has been limited because: (1) only a few cryodetection mass spectrometers systems exist in the world, (2) even though the detector technology has existed for nearly 20 years, cryodetection mass spectrometry is still in its infancy in terms of development, (3) limited data has been acquired and published demonstrating the advan-

tages of the cryodetection MS, (4) the detectors have a high maintenance cost, (5) cryodetectors, especially the calorimeter types, have a relatively long response time on order of microseconds. Even though the response time is shorter for STJs (≤1 μs), this can lead to reduced resolution at lower m/z, and finally, (6) the energy resolution of the STJ is limited to charge state determinations of about four. In addition, we and others have also observed a difference in the energy measured at the STJ due to the chemical nature of analyte [22].

The purpose of the current work is to further investigate the technology of cryodetection MALDI TOF MS for the analysis of polymers such as polystyrene and PMMA, to investigate certain aspects of the underlying chemistry and physics of the MALDI process above 150 kDa, and to assess the capability of the cryodetector mass spectrometer to determine the molecular weight and polydispersity of polystyrene into the mega Dalton mass range. Before this study, others have collected mass spectra of high mass polystyrene and PMMA [15, 28, 29]. The highest reported MALDI TOF distribution of polystyrene ions were observed at m/z 750 kTh for the +2 charge state of the 1.5 MDa polystyrene [15]. In out study, we collected mass spectra of both polystyrene and PMMA, but focused our work on the analysis of polystyrene.

Experimental

MALDI TOF Cryodetector Mass Spectrometer

The mass spectrometer used for this study was a Macromizer MALDI TOF system (COMET AG, Flamatt, Switzerland) equipped with a cryodetector that incorporates sixteen STJs [26]. This instrument utilizes a pulsed 337 nm nitrogen laser operated at 5 Hz (model VSL-337ND-S from Laser Science, Inc., Franklin, MA). The specified nonattenuated maximum laser power is 300 μJ/per pulse. It was typically set at 40% to 55% of the maximum value to achieve optimal resolution while maintaining good sensitivity. The laser power was increased for the higher mass polymers. The laser spot size was estimated to be ~60 μm X 80 μm by moving the MALDI plate a known distance and measuring the area of material removed by the laser.

The instrument was operated in positive ion mode with an acceleration voltage of 20 kV. The extraction delay time was optimized to be 11.4 μs for the 0.1–2 MTh mass range. The digitizer was incapable of processing a full mass range from 1 kDa to 5 MDa due to an undiagnosed hardware limitation; therefore, it was necessary to collect two or more spectra to cover the total range of interest. The Macromizer mass spectrometer has a "sequence scan" feature that can be programmed to sample a defined target area. This sampling feature coupled with signal averaging was used to reduce the effects of sample nonuniformity that typically occurs during sample drying on the MALDI plate.

Calibration

Calibration of the mass spectrometer from 100 kTh to 4 MTh was not accurate since calibrants have not been developed at such a high mass and over such an extensive mass range. We applied a mass calibration based on a polystyrene standard with a number average molecular weight (M_n) 400 kDa ± 20 kDa. This maximum M_n error of ±5% for 400 kDa polystyrene was provided by the manufacture [30]. This polymer sample was not an ideal calibrant since it is made up of many polymer chains with varying lengths and it was not known whether we were observing the true M_n. A three point calibration was applied using the doubly charged, singly charged, and singly charged bimolecular aggregate distributions, which were assumed to be centered at m/z 200 kTh, 400 kTh, and 800 kTh, respectively. The formation of bimolecular aggregates at 400 and 800 kTh would require an identical aggregation affinity for all the polymer chains in the distribution, which is unlikely to occur. However, since the PDI of the sample is very close to unity (see below), this error is minimized. The PMMA spectra were calibrated using a delay time of 8.25 μs and an immunoglobulin G protein standard with a molecular weight of 148.5 kDa.

Scatter Plots of the Energy Deposited Versus m/z

A major advantage of the cryodetector technology is the capability of distinguishing between individual ion charge states due to the energy dependence of the detector response. For example, an ion with a charge state of two should have twice the kinetic energy as the same ion with a charge state of one and thus the doubly charged ion should result in twice the energy deposited at the detector. Using a pulse counting mode, each of collision events on any of the sixteen STJ cryodetector pads is registered as a specific energy of an incident particle and these events can be displayed in a "scatter plot", a plot of the energy of each registered event versus m/z. Using the data manipulation software, ion events can also be processed over a select range of measured energies. In this manner, it is possible to select a energy range that would yield a mass spectrum due to primarily singly charged ions or doubly charged ions, . . . etc. Selecting the complete energy range, including all points, yields a mass spectrum of all charge states comparable to that obtained on a conventional mass spectrometer.

Acquisition of the Mass Spectra

The instrument control, acquisition and data processing software was version 1.23 (for JAVA 1.4.0) developed by COMET AG. The resulting mass spectra were generated by "binning", i.e., calculating the total energy of incident particles within a certain m/z (flight time) windows and plotting this value versus m/z. The spectra were smoothed by adjusting the size of the binning window, also called the "running class width parameter". An increased value for this parameter resulted in an improved S/N ratio [26], however, when the size of the bin was comparable to the time difference between two adjacent peaks, the resolution was reduced and the fine peak structure was lost.

Applied Biosystems Voyager DE sSTR TOF MS

The second mass spectrometer used in this work was an Applied Biosystems Voyager DE sSTR TOF MS equipped with a high mass high current detector (HCD) MCP (40 mm diameter). This instrument also utilizes a MALDI ion source with a 337 nm nitrogen laser. The instrument was operated in linear mode with an acceleration voltage of 25 kV and with an extraction delay time of 2 μs. Voyager software version 4.0 was used for instrument control and data acquisition and analysis.

Sample Preparation

Atactic polystyrene standards with M_n of 170 ± 8.5, 400 ± 20, 900 ± 90, and 2000 ± 200 kDa were commercially synthesized by Pressure Chemical Co. (Pittsburgh, PA). All-trans retinoic acid matrix was purchased from Sigma-Aldrich (St. Louis, MO) and stored in a cold, dark place. The THF solvent was distilled over Na metal to eliminate water which was found to have an adverse effect on the MALDI signal [15]. An optimal MALDI recipe for high mass polystyrene was developed by using a number of preparation methods based on early reports [28, 29]. The following combinations of matrix/solvent/cationizing agent were tested: dithranol or all-trans retinoic acid/THF or dichloromethane or toluene/silver nitrate or silver trifluoroacetate. An alternative solvent-free preparation method [31–33] was modified and also tried as described below.

The polystyrene samples that resulted in the best signal were prepared by combining 0.15 M all-trans retinoic acid matrix, near saturated solutions of polymers in dry THF and 1% by volume of a saturated solution of silver nitrate in absolute ethanol. The optimal concentration of the polymer in the resultant solution was determined experimentally in each case and was varied between a few nM to 1 μM depending on the M_n of the polymer (note: the polymer concentrations were calculated assuming that all of the polymer's molecules are of one single molecular weight equal to M_n). A 0.5–1.5 μL aliquot was then deposited on to the stainless steel MALDI plate and allowed to air dry.

For the solvent-free sample preparation [31–33], a small pellet of polystyrene was combined with the matrix in 10:1 to 1000:1 matrix-to-analyte ratio and 1% by mass of silver nitrate and pulverized in a mill (Tokken, Inc., Chiba, Japan) that consisted of a stainless steel plunger inside a plastic vial. The dry mixture was then pressed onto a MALDI plate with a spatula for MALDI analysis.

Atactic PMMA samples with M_n ranging from 7.6 to 153.7 kDa were from Polymer Laboratories (Shropshire, UK). Several MALDI recipes [14, 34, 35] with different matrices (2,5-dihydroxybenzoic acid (DHB), sinapinic acid, indole acrylic acid (IAA), α-cyano-4-hydroxy-cinnamic acid, etc.) with various solvents and salts were tested. The highest molecular weight PMMA results were obtained with the DHB matrix/acetone solvent/CsI salt combination [14] at a concentration of 17 μM.

Results and Discussion

Many factors affected the signal-to-noise (S/N) ratio for the polymer samples. For example, the highest MALDI signal level was observed near the edges of the sample spots, with a good signal often observed over a relatively large area up to ~0.5 mm in diameter. To achieve an optimal signal, the matrix-to-analyte ratio had to be greatly increased for the larger polymers. For example, for M_n of 170 kDa, 400 kDa, 900 kDa, and 2 MDa polystyrene, which is an increase in M_n by a factor of 1:2.4:5.3:11.8, respectively, the corresponding matrix/analyte dilution factor was increased by 1:1:5:320 times. For the M_n 2 MDa polystyrene sample, the best signal was observed when spotting down 3X the normal sample loading of 1.5 μL. For this sample it was also necessary to accumulate several thousands shots to achieve a S/N greater than 10.

The role of the solvent in the sample preparation of polystyrene can be examined by comparing the solvent-free results with the liquid phase results. In the case of polystyrene, the efficient mixing of matrix and analyte has been shown to be beneficial [38–40], but the formation of a solid solution is not required to generate a MALDI signal [36, 37]. Trimpin et al. have shown solvent-free MALDI mass spectra for polystyrene samples with molecular weights up to 100 kDa [31]. However, our solvent-free preparation procedure did not result in the observation of analyte peaks for the polymers studied. Since it has been shown that successful application of the solvent-free method requires a sufficient level of homogeneity [31, 41], we suspect that we did not achieve this high level of mixing with our system. Therefore, the lack of a solvent-free MALDI signal for polymers in our work could be attributed to inefficient mixing, insufficient separation of large polymer globules and/or possible breaking of polymer molecules during the pulverizing process.

The mass spectra obtained for M_n 170, 400, 900, and 2000 kDa polystyrene samples are shown in Figures 1, 2, 3, and 4. The elevated baseline observed in all of the spectra, and especially the higher molecular weight polystyrene samples and the PMMA, was attributed to chemical noise. As shown in Figures 1a, 2a, 3a, and 4a, the chemical noise levels increased in counts relative to the base peak signal for the 170, 400, 900, and 2000 kDa polystyrene samples, respectively. This elevated baseline was taken into account for the M_n, M_w, and the polydispersity calculations. The cause of the chemical

noise was not known, but several possibilities exist. A large amount of noise originates from the matrix itself, even above 100 kDa, as observed by a mass spectrum of a matrix and salt blank (i.e., no polymer). The matrix-only spectrum exhibited the characteristic baseline increase at lower m/z, and two broad bands of ion energies were observed from 0 to 15 keV for +1 ions and from ~15 to ~25 keV for multiply charged ions. These charged particles can be attributed to matrix impurities, matrix clusters, products of retinoic acid condensation (for the polystyrene samples) and other, likely light-induced, reactions. When collecting spectra from the polymer samples, the lower m/z signals can also be attributed to the fragmentation of the large polymer strands during sample preparation by agitation in solution [42] and in-source fragmentation from the absorption of the photons.

As described in the Experimental section, the Macromizer cryodetector mass spectrometer allowed for the measurement of the energy deposited at each STJ detector for each ion impact. After the acquisition, the "energy filtering" procedure can be applied to the data to generate a mass spectrum of the high or low energy regions. The mass spectra in Figures 1a–4a are the summation of all data points with no energy filtering and thus the data correspond to ions with all charge states. In Figure 1a, for instance, the peak at m/z 170,000 may be attributed to singly charged ions, doubly charge bimolecular ions, triply charged trimolecular ions, and so on. Using the scatter plot of energy deposited versus m/z in Figure 1b, it is possible to select a low charge state set of the data points to produce Figure 1c, which no longer shows the 5% relative abundance of the doubly charged ions at m/z 85 kTh, $[P + 2Ag]^{+2}$, where P = polymer. These "energy filtered" data are dominated by the singly charged monomolecular, bimolecular, trimolecular, tetramolecular, pentamolecular, and hexamolecular aggregates of 170 kDa polystyrene. When the higher data points in Figure 1b are processed, the abundance of the peaks in the spectrum in Figure 1d is assigned to multiply charged ions such as $[nP + 2Ag]^{+2}$, where $n = 1$–9. As determined from the observed m/z values in Figure 1d, the highest charge states obtained for the M_n 170 kDa polystyrene sample were the triply charged ions with the likely composition $[4P + 3Ag]^{+3}$ at m/z 227 kTh and $[5P + 3Ag]^{+3}$ at m/z 279 kTh etc. As can be seen from the scatter plot data, ~10% of the relative abundance of the monomolecular-, bimolecular-, trimolecular-, and tetramolecular aggregates was due to the +2 and/or higher charge states.

The data for M_n 400 kDa polystyrene are shown in Figure 2a–d, with Figure 2a representing the summation of all data points with no energy filtering. Applying a "low energy filter" to the scatter plot data produces the "low charge" state mass spectrum in Figure 2c, and applying a "high energy filter" to the scatter plot data produces the "high charge" state mass spectrum shown in Figure 2d. The low charge state mass spectrum in Figure 2c shows the expected monomolecular-,
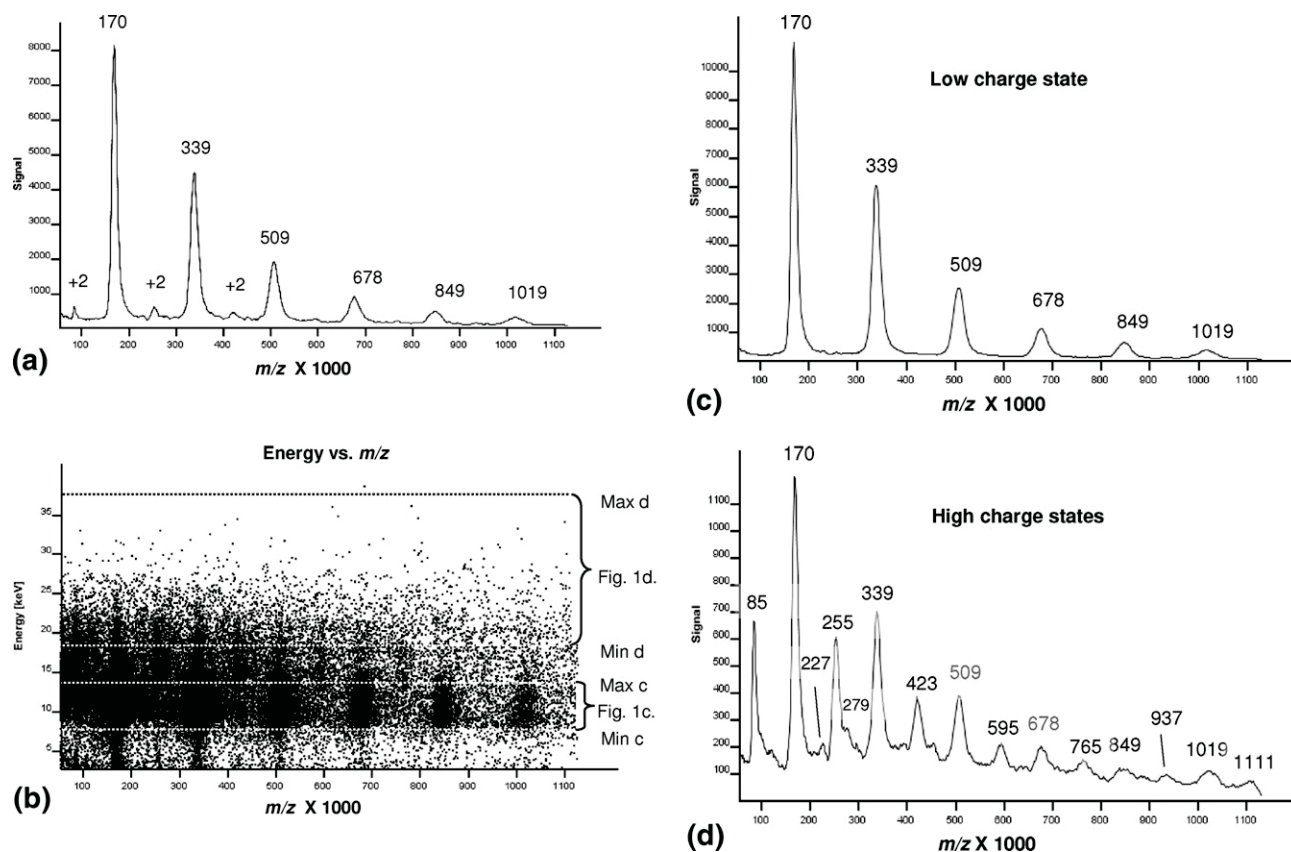
Figure 1. MALDI TOF cryodetector mass spectrum for polystyrene; M_n170,000; $M_w/M_n \leq 1.06$: (**a**) The mass spectrum acquired by processing all the ion events; (**b**) a scatter plot of the energy versus m/z recorded for the 16 channel cryodetector. A low energy region and a high energy region are selected to generate the mass spectra in (**c**) and (**d**), respectively. (**c**) Mass spectrum resulting from selecting only low energy ions between 7.1 and 14.0 keV. The spectrum is primarily made up of singly charged ions. There is some overlap with doubly charged ions at this level of energy filtering; (**d**) mass spectrum resulting by selecting the high energy ions between 18.2 and 37.0 keV. The spectrum is primarily made up of multiply charged ions with some contribution from singly charged ions.

bimolecular-, and trimolecular aggregates distributions with no doubly charged ion distribution. It is interesting to note that the tetramolecular- and pentamolecular aggregates were of lower relative abundance relative to the mass spectrum of the M_n 170 kDa polymer data in Figure 1c. Since we expect a cryodetector to show 100% detection efficiency at all m/z values, this could be attributed to the decreased efficiency of MALDI to generate singly charged aggregate ions for polystyrene and Ag^+ at high mass and a shift to the production of multiply charged ions. In the "high charge" state spectrum in Figure 2d, one can see an interesting aggregation pattern assigned to an even number of doubly charged polymer chains at 400, 804, 1200, and 1610 kTh for $[2P + 2Ag]^{+2}$, $[4P + 2Ag]^{+2}$, $[6P + 2Ag]^{+2}$, and $[8P + 2Ag]^{+2}$, respectively. We discuss this preferential even-numbered aggregate formation later in this section.

The mass spectrum for polystyrene with M_n 900 ± 90 kDa with no energy filtering is shown in Figure 3a. Observed in this spectrum are the singly- and doubly

charged ions at m/z 955 kTh and 475 kTh and the bimolecular aggregate at m/z 1907 kTh. The full set of all data points collected is shown in the scatter plot of the energy measured for each event versus m/z in Figure 3b. It is difficult to distinguish between the singly- and doubly charged energy bands due to the high density of points plotted. A slight increase of the measured energy as a function of m/z was observed for this sample. The exact nature of this phenomenon requires further investigation.

The mass spectrum in Figure 3c is the result of selecting only the low energy ions between 6.6 and 13.8 keV. The spectrum should be primarily made up of singly charged ions; however there is an overlap with a band of ions between the lower and higher regions that complicates distinguishing between the +1 and +2 energy bands. Metastable fragmentation of singly- or multi charged ions may account for some of the energy spread. In this case, the energy would be partitioned between the two fragments resulting in a lower measured energy than expected for the intact ion. The mass
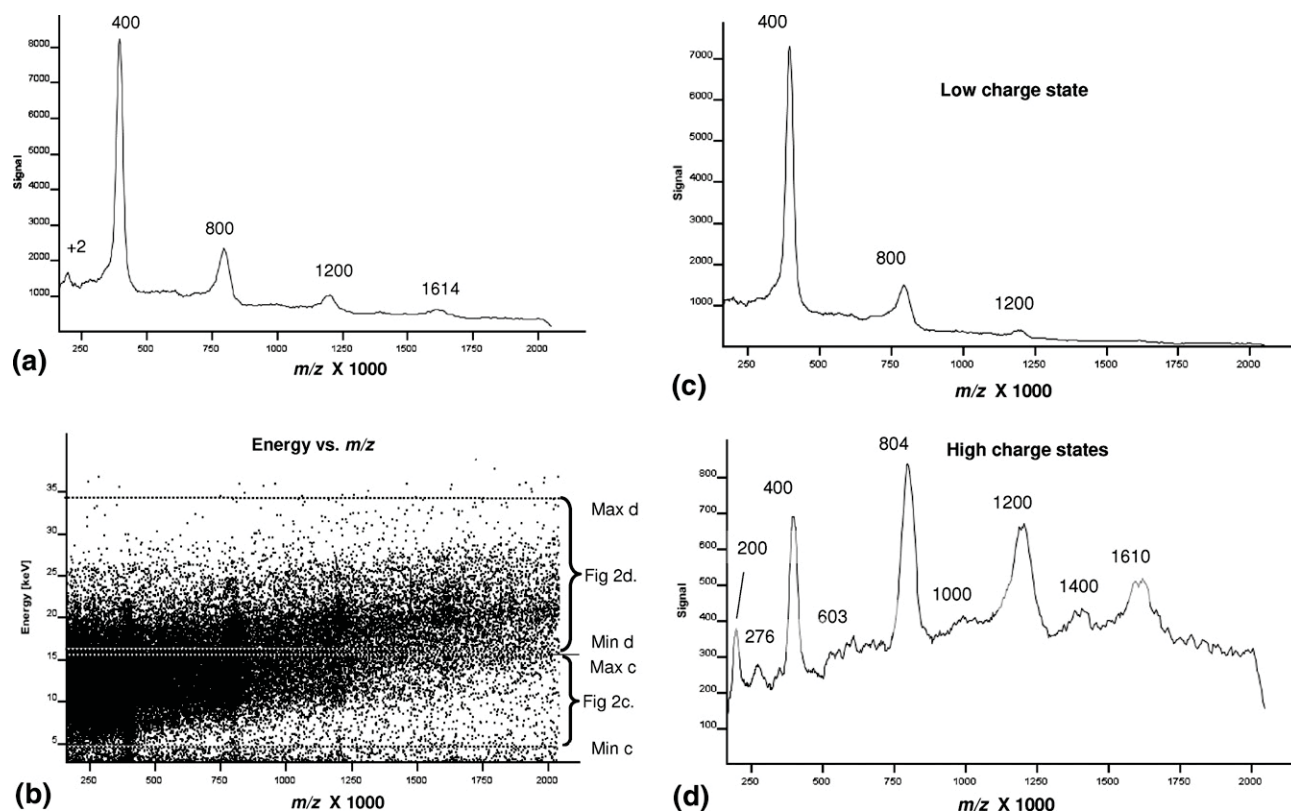
Figure 2. MALDI TOF cryodetector mass spectrum for polystyrene; M_n 400,000; $M_w/M_n \leq 1.06$: (**a**) The spectrum acquired by processing all the recorded ion events; (**b**) scatter plot of the collision events versus m/z recorded for the 16 channel cryodetector with an energy regions selected to generate the mass spectra in (**c**) and (**d**), respectively; (**c**) mass spectrum resulting from selecting for only low energy ions between 4.6 and 15.6 keV. The spectrum should be primarily made up of singly charged ions. Some doubly charged ion contribution is observed at this level of energy filtering; (**d**) mass spectrum resulting by selecting for only high energy ions between 16.3 and 34.8 keV. The spectrum should be primarily made up of doubly charged ions with some contribution from singly charged ions and a small amount of triply charged ions.

spectrum resulting by selecting for only high energy ions between 19.3 and 38.8 keV is shown in Figure 3d. The spectrum should be primarily made up of doubly charged and higher charge state ions, however, similar to the low energy ions, the overlap with the band of intermediate energies, complicates distinguishing the individual charge states. Note that the base peak at 900 kDa is made up of approximately equal amounts of singly charged monomers and doubly charged bimolecular aggregates. There is essentially no singly charged bimolecular aggregate present for the 900 kDa sample, as all of the biomolecular aggregates are doubly (or higher) charged. This, again, indicates that larger particles tend to acquire higher charge. Also, as in the M_n 400 kDa spectrum, we only observe the doubly charged ions for an even number of polystyrene adducts of $[2P + 2Ag]^{+2}$ and $[4P + 2Ag]^{+2}$.

The mass spectrum of polystyrene with M_n of 2 MDa is shown in Figure 4a with a m/z range 0.45–3 MTh and in Figure 4b with a m/z range 1.5–4.25 MTh. The "low charge" and "high charge" ion mass spectra were obtained by energy filtering the complete dataset in the scatter plot of Figure 4c, and these data are shown in

Figure 4d and e, respectively. The singly charged bimolecular aggregate distribution at 4 MTh in Figure 4d is not observed, as it is expected to be multiply charged. As shown in the mass spectrum of the higher charge state ions with energies between 27.2 and 45.7 keV in Figure 4e, the aggregates centered at m/z 2.2 MTh are, indeed, observed with a charge state greater than one. The primary formation of aggregate ions confirms the higher affinity of larger polymer strands to aggregate.

It should be noted that the assigned charge states discussed here are only tentative. Unlike photons, which deposit their energy in the bulk, the molecular particles cause energy absorption in the surface layer of the superconductor of a calorimeter or a STJ [43]. It was found that in the latter case, only a fraction of the total kinetic energy is detected, and the fraction of detected energy depends on the molecule type. Heavier molecules tend to deposit less of their kinetic energy. One of the possible explanations for the "missing" energy is fragmentation of the molecule hitting the detector and ejection of molecular fragments [43]. Hilton et al. found that for heavy ions, such as lysozyme and BSA, at large kinetic energies the energy fraction registered by a STJ
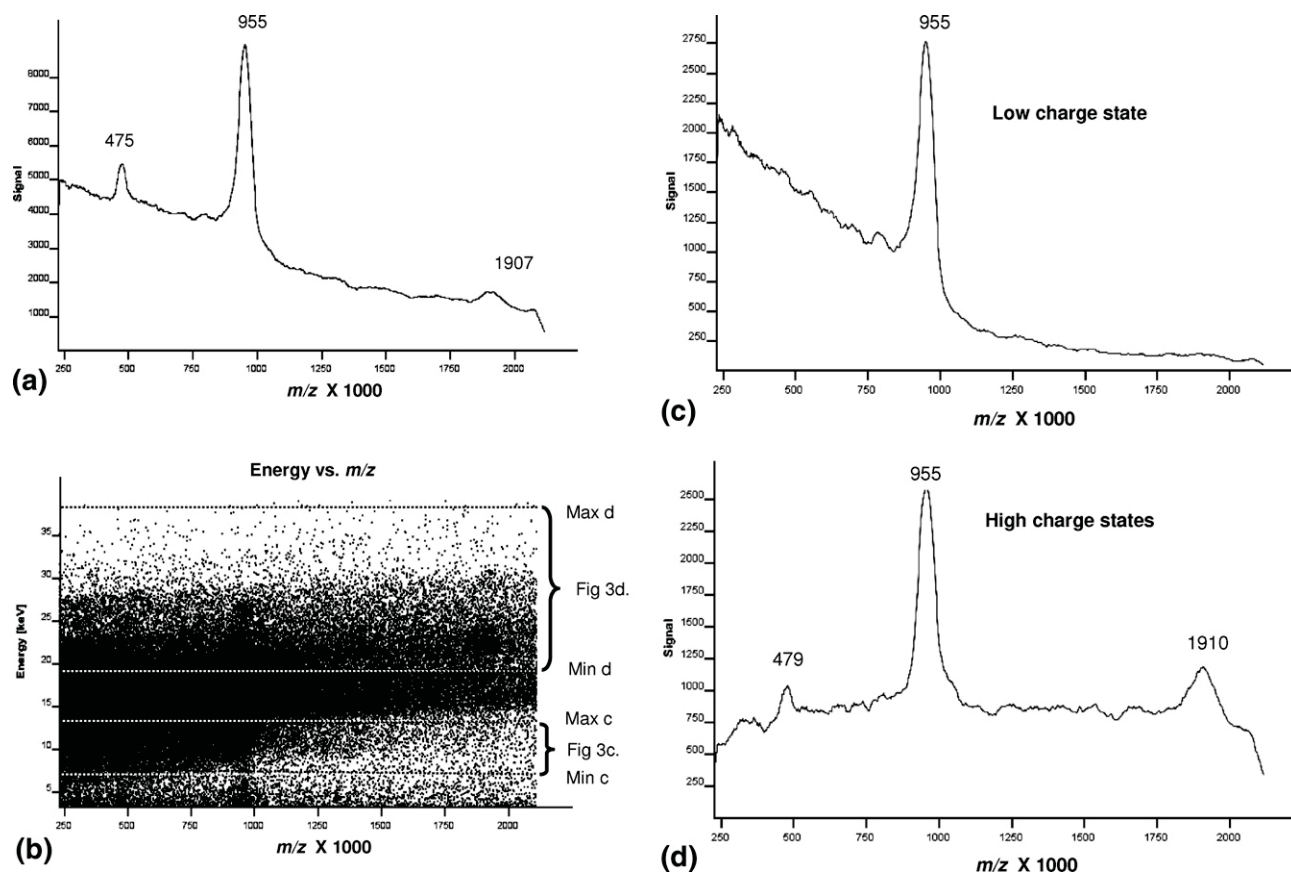
Figure 3. MALDI TOF cryodetector mass spectrum for polystyrene; M_n 900 kDa; $M_w/M_n \leq 1.06$: (**a**) No energy filtering; (**b**) scatter plot of the collision events versus m/z recorded for the 16 channel cryodetector with an energy regions selected to generate the mass spectra; (**c**) mass spectrum resulting from selecting for only low energy ions between 6.6 and 13.8 keV. The spectrum should be mostly made up of singly charged ions. The overlap with the band of chemical noise complicates discerning of individual energy bands. (**d**) mass spectrum resulting by selecting for only high energy ions between 19.30 and 38.8 keV. The spectrum should be primarily made up of doubly and higher charged ions, however, similarly with the low energy ions; the overlap with the band of "chemical noise" complicates discerning of individual energy bands.

cryodetector approaches 0.54 [43]. Thus, for the acceleration voltage 20 kV used in our experiments, the singly charged ion can be expected to be registered at and around 11 keV. This value is consistent with our data: for smaller polymers, the singly charged and doubly charged bands are centered at ~10–12 keV and 15–22 keV, respectively (Figures 1b, 2b, 3b). However, as can be noted in Figure 4c for the M_n 2MDa polymer, the presumed +1 and +2 bands in this case are centered at energy values which are noticeably higher, ~17 keV and 30 keV, respectively. This occurs even though Hilton *et al.* found that the larger particles tend to deposit lower energy [43]. Based on our data, the peak observed at 2.2 MTh for the M_n 2 MDa polystyrene sample was assigned to be primarily due to doubly charged ~4 MDa bimolecular aggregates. An unambiguous correlation between the energy registered by our cryodetector system and the charge state of an ion requires more study. A better understanding of the relationship between energy deposited at the STJ detectors and the chemical nature of the analyte as well as

improved energy resolving power is required to make a charge state assignment with a high level of confidence.

Compared with the studies of high mass polystyrene by Schriemer and Li [15], our data revealed enhanced high m/z signals that we believe are primarily due to the advantage of using a cryodetector. In their studies, using a conventional ionizing detector, the +2 or +3 charge states are the most abundant distributions in the spectrum for $M_n/z > 150,000$. Our data obtained on a MALDI TOF mass spectrometer with a conventional ionizing detector indicated a similar trend. As can be seen in Figure 5, the intensities of the unassociated polymer and bimolecular aggregate peaks of the M_n 170 kDa polystyrene at ~170 and ~340 kTh correspondingly, are nearly 10:1 ratio. In contrast to these data, the cryodetector data indicated this ratio to be ~2:1 and revealed a favored formation of multimeric aggregates with molecular weight up to 1 MDa or greater. These data demonstrated the improved detection of high m/z ions by the cryodetector and the uniqueness of the MALDI technique, which remains the most convenient,
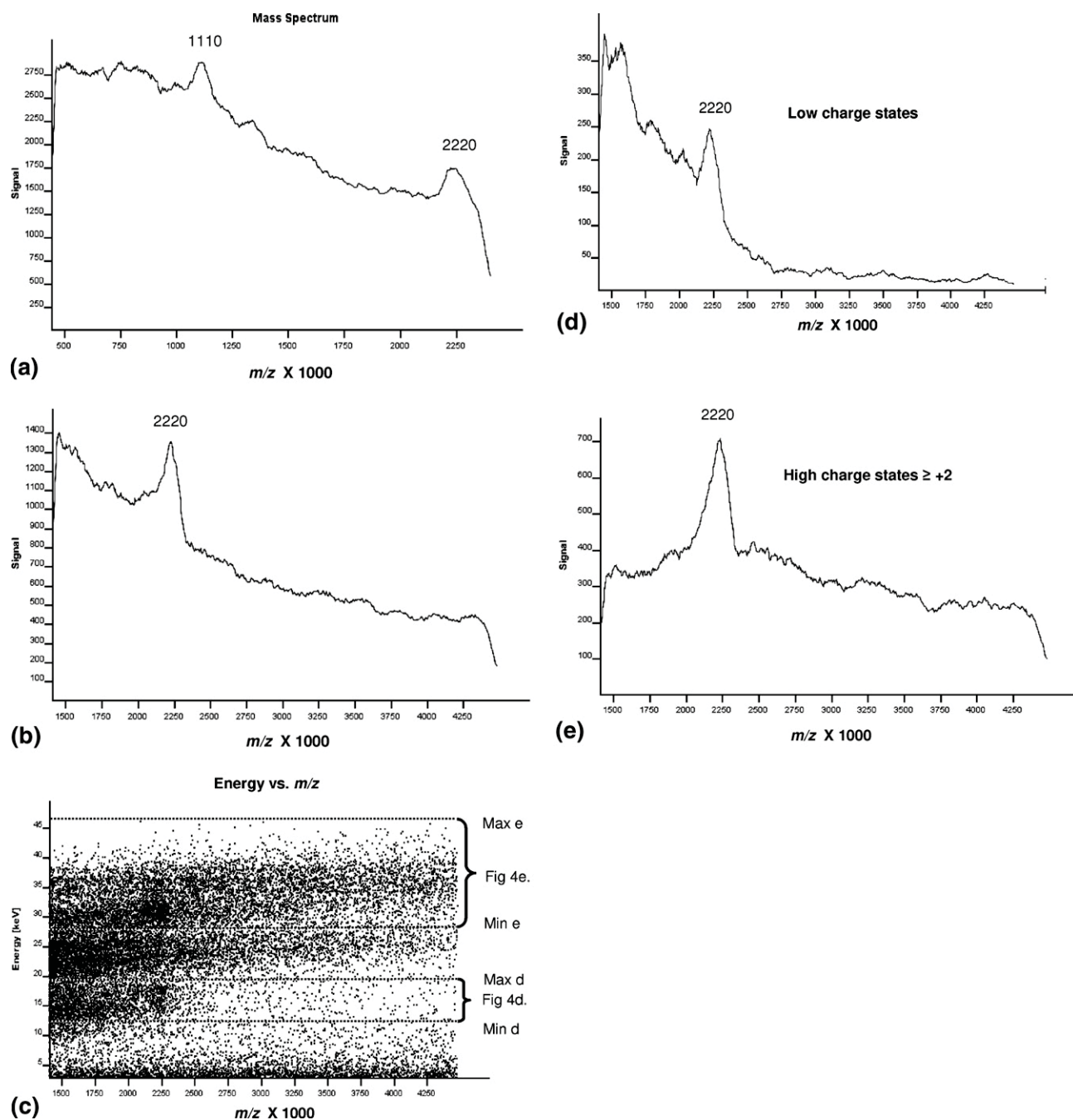
Figure 4. MALDI TOF cryodetector mass spectrum for polystyrene; M_n 2 MDa; $M_w/M_n \leq 1.30$: (**a**) No energy filtering, "low" mass range; (**b**) no energy filtering, "high" mass range; (**c**) scatter plot of the collision events versus m/z recorded for the 16 channel cryodetector with an energy regions selected to generate the mass spectrum in (**d**) and (**e**), respectively; (**d**) mass spectrum resulting from selecting for only low energy ions between 12.0 and 19.0 keV. The spectrum should be primarily made up of singly charged ions. Some multiply charged ion contribution may be observed at this level of energy filtering; (**e**) mass spectrum resulting by selecting for only high energy ions between 27.2 and 45.7 keV. The spectrum should be primarily made up of doubly and higher charged ions.

straight forward method to the generation low charged state heavy ions, even in the mega dalton range.

Conventional MALDI TOF mass spectrometers have not produced accurate PDI values at high m/z, which is primarily believed to be due to the reduction of signal at high mass due to the MALDI process and the MCP detectors. Researchers have instead relied on other methods such as laser light scattering and thermal field flow fractionation [44]. We wanted to explore the possibility of obtaining improved PDI values for our polystyrene sample by using cryodetector MS. From the polystyrene mass spectra, we calculated values of M_n,
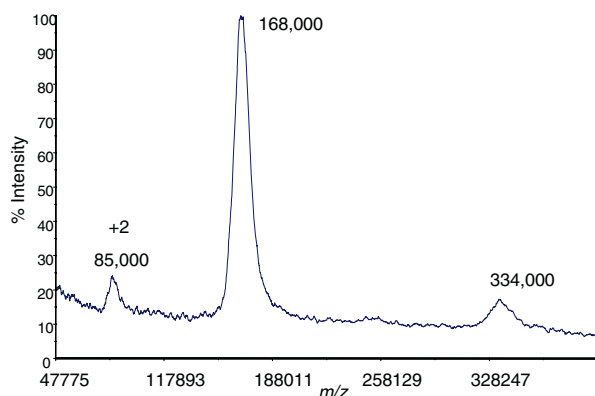
Figure 5. MALDI TOF mass spectrum for polystyrene with M_n 170,000 obtained on Voyager STR instrument showing the doubly charged, singly charged, and bimolecular aggregate distribution at m/z 85 kTh, 168 kTh, and 334 kTh respectively. A 101 point smoothing algorithm was applied to these data.

weight average molecular weight (M_w), and polydispersity index (PDI = M_w/M_n) and the results are shown in Table 1. Equations 1 and 2 were used to calculate M_n and M_w where N_i and M_i are signal

$$M_n = \frac{\sum N_i M_i}{\sum N_i} \qquad (1)$$

$$M_w = \frac{\sum N_i M_i^2}{\sum N_i M_i} \qquad (2)$$

intensity and mass at point i, respectively. Only the peaks resulting from the contribution from singly charged ions, obtained by the "energy filtering" procedure, were employed for these calculations. The ions in the mass range used for these calculations were all ≥3% of the relative abundance for a given distribution. The polydispersities determined were within the broad range provided by the manufacturer (e.g., 1.00–1.06 for M_n 170 kDa) as shown in the PDI column of Table 1. The manufacturer's M_n, M_w, and PDI values were estimated based on the combination of methods such as fractionation, examination of sedimentation profile, intrinsic viscosity measurements, and GPC. Shortt [45] determined PDI values for similar polystyrene samples from

the same manufacture to be 1.00,096 ± 0.00,004 using a laser light scattering (LLS) technique. His results are much closer to unity and consistent with our narrower distribution as shown by our cryodetector PDI data in Table 1.

We also collected MALDI TOF mass spectra for a series of PMMA samples with molecular weights varying from 7.6 to 153.7 kDa. All of the spectra had a similar appearance with a baseline that increased at low m/z for the higher MW samples. A representative spectrum of the M_n 153.7 kDa sample is shown in the Supplemental Materials section. The highest observed m/z for PMMA was the doubly charged tetramolecular aggregate of M_n 153.7 kDa polymer with a molecular weight of ~598.0 kDa, at 299.0 kTh. Energy filtering the scatter plot data and analyzing the resultant spectra, as described above, allowed us to identify the bands of primarily singly and doubly charged ions. For example, the singly charged ions at m/z 448.8, 298.0, and 146.6 were found to correspond to a M_n 153.7 kDa PMMA trimer, dimer, and nonaggregated monomer, and the doubly charged ions at m/z 299.0, 223.8, 149.6, and 74.3 correspond to the tetramer, trimer, dimer, and monomer, respectively. A small amount of triply charged dimer could also be observed at m/z 105.0.

Our results demonstrate the highest observed m/z for PMMA, the doubly charged, presumably, tetramolecular aggregate at ~598.0 kDa (299.0 kTh), which is higher than any of the PMMA results previously reported for MALDI TOF MS studies with conventional detectors. The sample preparation was critical for the PMMA polymer and a poorly prepared sample could render the cryodetection technology to be of little advantage. The best results obtained for the PMMA samples were found to give a significantly lower S/N level with similar acquisition times to those obtained for the polystyrene samples. This is consistent with the data reported, which indicate a higher MALDI efficiency for the polystyrene compared with other high-mass synthetic polymers. In our studies, there is approximately a tenfold decrease in the detection limit of polystyrene compared with PMMA with any combinations of matrix compounds and salt [14]. The reason for the signal improvement is unclear, but it is most likely due to polysty-

Table 1. The M_n, M_w and polydispersity index (PDI) found for four polystyrene samples using the MALDI TOF mass spectrometer with cryodetection

M_n, kDa (PDI)*	Determined base peak m/z of polymer distribution, kTh				Determined M_n, kDa	Determined M_w, kDa	Determined PDI
	P^+	$2P^+$	$3P^+$	$4P^+$			
170 (≤1.06)	170	339	509	678	174 ± 9	180	1.009
400 (≤1.06)	400	800	1200	1610	394 ± 20	396	1.004
900 (≤1.06)	955	1910	—	—	950 ± 95	960	1.003
2000 (≤1.30)	2240	4270	—	—	2200 ± 220	2200	1.003

*PDI values are from Pressure Chemical, Inc. (Pittsburgh, PA) were given as a range, e.g., 1.00–1.06. The true PDI was not known.

rene itself and/or the matrix/silver combination used compared with the other polymer/matrix combinations.

Both steps of the MALDI process, laser ablation and gas-phase reactions, are expected to be very efficient in the case of the polystyrene/all-trans retinoic acid/silver nitrate combination. For the ablation step, we indeed observed unusually high sample removal rate when all-trans retinoic acid was used as matrix. The laser power used in our experiments was typically sufficient to ablate the sample to the metal plate after 10 to 30 shots. Such a high rate of sample removal was not observed with the other matrix compounds in our studies. This observation suggests that an exceptionally high ablation efficiency [46] is required to observe a MALDI signal from these heavy polymers.

Another crucial factor in the MALDI process is the energetics of ion formation. In the case of polystyrene, the lack of basic groups makes charge acquisition via proton transfer inefficient. However, the presence of phenyl rings enables π-complexation of metal cations such as Ag^+ or Cu^+. The formation of these complexes is nearly thermoneutral [47]. Consequently, the matrices such as dithranol with low cation affinity were found to be very efficient for polymer analysis [6].

In the case of polystyrene, a metal bound complex can potentially form in either the liquid/solid or the gas phase. Others have shown evidence of in-plume cationization of the polystyrene molecules [38, 48–50]. Cationization energetics should be nearly equal for small or large polymer molecules. This strongly suggests that the key factor in determining the amount of polystyrene ions generated by MALDI is not the ionization efficiency, but rather the efficiency of the ablation process, i.e., the transfer of the polystyrene molecules or ions into the gas phase. Similar efficiency can also be expected from all-cis retinoic acid, which was reported to be an even better matrix than all-trans isomer for analysis of dendrimers [51].

One of the prominent features in the spectra discussed above is the abundance of polymer aggregates, similar to those observed by Ohkubo et al. [23]. In the case of M_n 400 kDa polystyrene, the doubly charged aggregates form up to octamolecular ions at 1.60 MDa, as can be seen in Figure 2d. For the M_n 170 kDa polystyrene, the doubly charged aggregates form up to a dodecamolecular ion at 1.02 MTh, as can be seen in Figure 1d. Understanding the underlying principles for the formation of such aggregates is of interest in mass spectrometry as well as in general. Such knowledge could allow for a better understanding of the association of bio-polymers, e.g., DNA packing and protein folding. The MALDI-TOF MS data could provide an additional means of measuring the molecular weight distribution of a polymer to those commonly employed in polymer science, e.g., the determination of the radius of gyration R_G and the hydrodynamic radius R_H (numerically equal to R_G) [52].

Caution should be used when interpreting MALDI mass spectra since the behavior of polymer chains is greatly affected by the presence of the MALDI matrix. The amount of chain contraction and collapse into a globule in a polymer/matrix/solvent system is governed by the polymer/matrix and polymer/solvent interactions. The final shape of the polymer molecule as well as the degree to which polymer association occurs will be dependent primarily on the matrix/polymer interaction during the final stages of evaporation [53]. Such studies may provide useful information if aggregates pre-exist in the solution phase before mixing and are stable enough to remain intact throughout the MALDI sample preparation and laser ablation.

In the case of polystyrene aggregation, it is likely the multimers existed in the MALDI sample and then were transferred to the gas phase. The energy filtering capability of the cryodetector enabled us to estimate the relative amounts of unassociated polymer strands versus those associated into multimeric complexes. As expected, the results show that the degree of association of polystyrene increases with the size of the polymer. In the series M_n 400, 900, and 2000 kDa, the percentage of unassociated polymer (strands of both +1 and +2 charges) was found to be ~40%, 29%, and 10%, respectively. This suggests that for the M_n 2 MDa sample, the actual species transferred into the gas phase are mostly multimers (90% by mol.) of ~4 MDa or higher molecular weight. The high molecular weight of these aggregates may have partially contributed to the disproportionate increase in the matrix/substrate ratio necessary for an optimal signal as discussed above in the Experimental section.

In the present study, an interesting multimeric pattern was observed for the 400 and 900 kDa samples and, to some extent, the 170 kDa polystyrene samples. As can be seen in Figure 2d, for the M_n 400 kDa polystyrene, the major peaks observed in the spectrum are bimolecular, tetramolecular, hexamolecular, and octamolecular aggregates carrying two charges. The doubly charged trimolecular, pentamolecular, and heptamolecular aggregates peaks are considerably less abundant. For the M_n 900 kDa polystyrene, only the doubly charged bimolecular and tetramolecular, but not the trimolecular or pentamolecular aggregates are formed (Figure 3d). Such preferred even- versus odd-numbered aggregation is not observed for the singly charged ions, where uniform, exponential decrease in n-molecular aggregate amount as a function of n is observed (Figures 1b, 2b). A number of explanations of this effect can be suggested. It can be hypothesized that the preferential formation of an even-number aggregates results from preferential initial dimerization. The bimolecular aggregates can be formed in either condensed phase during sample preparation or in the gas phase. The structure of such bimolecular complexes could be similar to the gas-phase M_2Bz_3 sandwich structures of transition metals benzyl complexes postulated by Kurikawa et al. [54]. Each complex incorporates two silver ions and carries the +2 charge. If three of the phenyl rings belong to two different polystyrene chains,

then the resultant complex would be $[2P+2Ag]^{+2}$. Further aggregation of these complexes either in solution or in the gas phase and possible partial charge reduction during the MALDI process would result in the formation of doubly charged tetramolecular, hexamolecular, and other even numbered aggregates.

The binding of two Ag^+ ions to three phenyl rings in the postulated complexes would involve η^6 and η^2 binding to the outer and inner phenyl rings of the polymer(s), respectively. The η^2 benzyl complex, though unusual, is indeed documented for the Ag^+ [55]. The Ag^+ ion has d^{10} configuration, therefore, in the proposed $[(\eta^6\text{-Ph})Ag(\eta^2,\eta^2\text{-Ph})Ag(\eta^6\text{-Ph})]^{+2}$ complex both Ag metal centers have a closed-shell 18 electron count. The energetic effects of the complexation, however, are going to be negated by the disruption of aromaticity in the middle phenyl ring. This is consistent with the reported thermoneutrality of formation of a π-complex of Ag^+ with the phenyl ring of the polystyrene [47]. Bimolecular aggregation could also come about from the binding of two Ag^+ cations to two polystyrene chains at different locations.

It should be noted that the proposed scheme is a suggested possibility, and the origin of the phenomenon of preferred even-numbered aggregates formation for the polystyrene with silver cation requires additional study. Several factors may alter the observed multimeric pattern such as different cations (Ag(II) or Cu(I)), substituents on the phenyl ring or along the main chain in polystyrene, polymer's tacticity, ... etc. The investigation of these effects may reveal important clues about the mechanism of the MALDI process for polystyrene, as well as the MALDI process in general.

Conclusions

A MALDI TOF mass spectrometer which incorporates a STJ cryodetector can be used to increase the sensitivity at high mass and allow for an improved signal response for polymers such as PMMA and polystyrene. Distributions of PMMA with a M_n 153.7 kDa were observed as high as the trimolecular aggregate distribution at 448.7 kDa. Polystyrene, singly charged monomer ion distributions and doubly charge aggregates were observed up to ~2.2 MTh. Compared to a conventional ionizing detector, the cryodetector has revealed that there is indeed a higher proportion of high m/z (low z) ions produced in the MALDI process than previously reported for polystyrene [15] and these broad peaks can be made up of more than one charge state.

The cryodetector system allowed for the determination of charge state by measuring the energy deposited at the STJ detector elements for each ion collision event. With the energy resolution obtainable by current instrument, a charge state up to three was distinguishable for polystyrene ions, but it is possible to observe higher charge states in the scatter plots. By summing a band of energies in the scatter plots of energy versus m/z, it is possible to create a mass spectrum showing only select charge states. In this fashion it is possible to determine the charge state make-up of a peak. Such information is not available when using conventional ionizing detectors.

Since the cryodetector theoretically has 100% detection efficiency at any m/z, it was possible to evaluate the high m/z limitations of the MALDI technique for polystyrene. To lift and fly these high molecular weight polystyrene polymers efficiently, a greatly increased matrix/analyte ratio was required. As a result, even when an optimal signal for the higher molecular weight samples is achieved, the signal intensity is typically lower than that for lower molecular weight samples. Optimization of the sample preparation techniques, as well as the thorough purification of solvents and matrix can further improve the signal intensity. Our data indicate that the key criterion for an ultra high mass analysis of polystyrene may be the use of a matrix with high ablation efficiency.

The ability to detect low charge state, high mass polystyrene ions into the Mega Dalton mass range with the STJ cryodetector provides researchers with a new tool to mass analyze these samples and to study processes which involve these macromolecules. For example, one could characterize polymers by cryodetector mass spectrometry at high molecular weights to gain insight about a synthetic process. In another example, one could study the aging/degradation of very large polymers such as high molecular weight polyethylene used for hip implants [56] or the thermal or chemical degradation of polymers of virtually any molecular mass [57]. With further work, mass spectrometry analysis using a cryodetector may provide a new fast and convenient tool to determine the PDI of large polymers. In addition to the analysis of synthetic polymers, promising applications for MALDI TOF MS with STJ cryodetection can be directed at studying macromolecular complexes found in nature.

Acknowledgments

References

1. Tanaka, K.; Ido, Y.; Yoshida Y.; Yoshida T. *Proceedings of the Second Japan-China Joint Symposium on Mass Spectrometry*; Osaka, Japan, September 1987.
2. Tanaka, K.; Waki, H.; Ido, Y.; Akita, S.; Yoshida, Y.; Yohida, T. Protein and Polymer Analyses up to m/z 100,000 by Laser Ionization Time-of-Flight Mass Spectrometry. *Rapid Commun. Mass Spectrom.* **1988,** *2*(*8*), 151–153.
3. Karas, M.; Hillenkamp, F. Laser desorption ionization of proteins with molecular masses exceeding 10,000 daltons. *Anal. Chem.* **1988,** *60*, 2299–2301.
4. Zenobi, R.; Breuker, K.; Knochenmuss, R.; Lehmann, E.; Stevenson, E. Fundamentals and Applications of MALDI Mass Spectrometry. *Adv. Mass Spectrom.* **2001,** *15,* 143–149.
5. Knochenmuss, R.; Zenobi, R. MALDI Ionization: The Role of In-Plume Processes. *Chem. Rev.* **2003,** *103*(2), 441–452.
6. Knochenmuss, R. Ion Formation Mechanisms in UV-MALDI. *Analyst (Cambridge, UK)* **2006,** *131*(9), 966–986.

7. Johnston, P. M.; Bergman, M. R.; Zakheim, D. *Chem. Phys.* **1975,** *62*(2500
8. Hillenkamp, F.; Karas, M.; Beavis, R. C.; Chait, B. T. Matrix-Assisted Laser Desorption/Ionization Mass Spectrometry of Biopolymers. *Anal. Chem.* **1991,** *63*(24), 1193A–1203A.
9. Zenobi, R.; Knochenmuss, R. Ion Formation in MALDI Mass Spectrometry. *Mass Spectrom. Rev.* **1999,** *17*(5), 337–366.
10. Westmacott, G.; Ens, W.; Standing, K. G. Secondary Ion and Electron Yield Measurements for Surfaces Bombarded with Large Molecular Ions. *Nucl. Instrum Methods Phys. Res. B* **1996,** *108*(3), 282–289.
11. Brunelle, A.; Chaurand, P.; Della-Negra, S.; Le Beyec, Y.; Parilis, E. Secondary Electron Emission Yields from a CsI Surface Under Impacts of Large Molecules at Low Velocities (5 ∗ 103-7 ∗ 104 ms-1). *Rapid Commun. Mass Spectrom.* **1997,** *11*(4), 353–362.
12. Beuhler, R. J.; Friedman, L. Threshold Studies of Secondary Electron Emission Induced by Macro-Ion Impact on Solid Surfaces. *Nucl. Instrum. Methods* **1980,** *170*(1/3), 309–315.
13. Twerenbold, D.; Gerber, D. D.; Gritti, D.; Gonin, Y.; Netuschill, A. A.; Rossel, A.; Schenker, D.; Vuilleumier, J.-L. Single Molecule Detector for Mass Spectrometry with Mass Independent Detection Efficiency. *Proteomics* **2001,** *1*(1), 66–69.
14. Danis, P. O.; Karr, D. E. A Facile Sample Preparation for the Analysis of Synthetic Organic Polymers by Matrix-Assisted Laser Desorption/Ionization. *Org. Mass Spectrom.* **1993,** *28*(8), 923–925.
15. Schriemer, D.C.; Li, L. Detection of High Molecular Weight Narrow Polydisperse Polymers up to 1.5 Million Daltons by MALDI Mass Spectrometry. *Anal. Chem.* **1996,** *68*(17), 2721–2725.
16. Nelson, R. W.; Dogruel, D.; Williams, P. Detection of human IgM at *m/z* approximately 1 MDa. *Rapid Commun. Mass Spectrom.* **1995,** *9*(7), 625.
17. Wenzel, R. J.; Kern, S.; Zenobi, R. *Proceedings of the American Society for the Mass Spectrometry conference*, Indianapolis, IN, June 2007.
18. Westfall, M. S.; Scalf, M.; Smith, L. M. Extended Mass Range Ion Detectors for Time-of-Flight Mass Analysis. *Proceedings of the American Society for the Mass Spectrometry Conference*, Indianapolis, IN, June 2007.
19. Esposito, E.; Cristiano, R.; Pagano, S.; Perez de Lara, D.; Twerenbold, D. Fast Josephson Cryodetector for Time of Flight Mass Spectrometry. *Physica C (The Netherlands)* **2002,** *372/376*(Pt. 1), 423–426.
20. Gervasio, G.; Gerber, D.; Gritti, D. D.; Gonin, D.; Twerenbold, D.; Vuilleumier, J. L. Aluminium Junctions as Macromolecule Detectors and Comparison with Ionizing Detectors. *Nucl. Instrum. Methods Phys. Res. A* **2000,** *444*(1/2), 389–394.
21. Frank, M.; Mears, C. A.; Labov, S. E.; Benner, W. H. (The Regents of the University of California, USA). 1999, p. 8. Ultra-High-Mass Spectrometry with Charge Discrimination Using Cryogenic Detectors. U.S. Patent.
22. Frank, M.; Labov, S .E.; Westmacott, G.; Benner, W. H. Energy-Sensitive Cryogenic Detectors for High-Mass Biomolecule Mass Spectrometry. *Mass Spectrom. Rev.* **1999,** *18*(3/4), 155–186.
23. Ohkubo, M.; Shigeri, Y.; Kinumi, T.; Saito, N.; Ukibe, M.; Chen, Y. E.; Kushino, A.; Kurokawa, A.; Sato, H.; Ichimura, S. Fragmentation Analysis by Superconducting Ion Detectors in Matrix-Assisted Laser Desorption/Ionization (MALDI). *Nucl. Instrum. Methods Phys. Res. A* **2006,** *559*(2), 779–781.
24. Clark, C. G.; Andreitchenko, E. V.; Wenzel, R. J.; Zenobi, R.; Muellen, K. Phenylene Propellers and Dendrimers: Molecular Recognition Motifs from 2 to 25 nm. *Proceedings of the 231st ACS National Meeting, (Abstracts of Papers)*; Atlanta, GA, March, 2006; p PMSE-139.
25. Nazabal, A.; Wenzel, R. J.; Zenobi, R. Immunoassays with Direct Mass Spectrometric Detection. *Anal. Chem.* **2006,** *78*(11), 3562–3570.
26. Wenzel, R. J.; Matter, U.; Schultheis, L.; Zenobi, R. Analysis of Mega Dalton Ions Using Cryodetection MALDI Time-of-Flight Mass Spectrometry. *Anal. Chem.* **2005,** *77*(14), 4329–4337.
27. Kraus, H. Cryogenic Detectors and Their Application to Mass Spectrometry. *Int. J. Mass Spectrom.* **2002,** *215*(1/3), 45–58.
28. Belu, A. M.; DeSimone, J. M.; Linton, R. W.; Lange, G. W.; Friedman, R. M. Evaluation of Matrix-Assisted Laser Desorption Ionization Mass Spectrometry for Polymer Characterization. *J. Am. Soc. Mass Spectrom.* **1996,** *7*(1), 11–24.
29. Lim, H.; Lee, Y.; Han, S.; Yoo, Y.; Kim, K.-J. Investigation of Polystyrene, Polyisoprene, and Poly(2-Vinylpyridine) Using Matrix-Assisted laser Desorption/Ionization Time-of-Flight Mass Spectrometry. *Bull. Korea Chem. Soc.* **1999,** *20*(7), 853–856.
30. Rosen, L. J. Pressure Chemicals, Chairman and CEO. *Personal communication.*, Pittsburgh, PA, 2006.
31. Trimpin, S.; Rouhanipour, A.; Az, R.; Rader, H. J.; Mullen, K. New Aspects in Matrix-Assisted Laser Desorption/Ionization Time-of-Flight Mass Spectrometry: A Universal Solvent-Free Sample Preparation. *Rapid Commun. Mass Spectrom.* **2001,** *15*(15), 1364–1373.
32. Trimpin, S.; Deinzer, M. L. Solvent-Free MALDI-MS for the Analysis of Biological Samples via a Mini-Ball Mill Approach. *J. Am. Soc. Mass Spectrom.* **2005,** *16*(4), 542–547.
33. Hanton, S. D.; Parees, D. M. Extending the Solvent-Free MALDI Sample Preparation Method. *J. Am. Soc. Mass Spectrom.* **2005,** *16*(1), 90–93.
34. Hunt, K. H.; Crossman, M. C.; Haddleton, D. M.; Lloyd, P.M.; Derrick, P. J. Polymerization of Methyl methacrylate with Tert-Butyl-Lithium and Tri-Isobutyl Aluminum in Toluene: Mechanism of Initiation and Termination by Matrix-Assisted Laser Desorption Ionization Time-of-Flight MSass spectrometry (MALDI TOF MS). *Macromol. Rapid Commun.* **1995,** *16*(10), 725–732.
35. Jackson, C.; Larsen, B.; McEwen, C. Comparison of Most Probable Peak Values As Measured for Polymer Distributions by MALDI Mass Spectrometry and by Size Exclusion Chromatography. *Anal. Chem.* **1996,** *68*(8), 1303–1308.
36. Bauer, B. J.; Byrd, H. C. M.; Guttman, C. M. Small Angle Neutron Scattering Measurements of Synthetic Polymer Dispersions in Matrix-Assisted Laser Desorption/Ionization Matrixes. *Rapid Commun. Mass Spectrom.* **2002,** *16*(15), 1494–1500.
37. Bauer, B.J.; Guttman, C.M.; Liu, D.; Blair, W. R. Tri-α-Naphthylbenzene as a Crystalline or Glassy Matrix for Matrix-Assisted Laser Desorption/Ionization: A Model System for the Study of Effects of Dispersion of Polymer Samples at a Molecular Level. *Rapid Commun. Mass Spectrom.* **2002,** *16*(12), 192–1198.
38. Erb, W. J.; Hanton, S. D.; Owens, K. G. A Study of Gas-Phase Cationization in Matrix-Assisted Laser Desorption/Ionization Time-of-Flight Mass Spectrometry. *Rapid Commun. Mass Spectrom.* **2006,** *20*(14), 2165–2169.
39. Hoteling, A. J.; Mourey, T. H.; Owens, K. G. Importance of Solubility in the Sample Preparation of Poly(Ethylene Terephthalate) for MALDI TOFMS. *Anal. Chem.* **2005,** *77*(3), 750–756.
40. Hoteling, A. J.; Erb, W. J.; Tyson, R. J.; Owens, K. G. Exploring the Importance of the Relative Solubility of Matrix and Analyte in MALDI Sample Preparation Using HPLC. *Anal. Chem.* **2004,** *76*(17), 5157–5164.
41. Hanton, S. D. S.; James, R. Investigating Time and Mass Effects in Solvent-Free MALDI Sample Preparation. *Proceedings of the American Society for the Mass Spectrometry Conference*, Indianapolis, IN, June 2007.
42. Berry, G. C.; Professor Emeritus. *Personal communication.*, Pittsburgh, PA, 2006.
43. Hilton, G. C.; Martinis, J. M.; Wollman, D. A.; Irwin, K. D.; Dulcie, L .L.; Gerber, D.; Gillevet, P. M.; Twerenbold, D. Impact Energy Measurement in Time-of-Flight Mass Spectrometry with Cryogenic Microcalorimeters. *Nature* **1998,** *391*(6668), 672–675.
44. Kassalainen, G. E.; Williams, S. K. R. Coupling Thermal Field-Flow Fractionation with Matrix-Assisted Laser Desorption/Ionization Time-of-Flight Mass Spectrometry for the Analysis of Synthetic Polymers. *Anal. Chem.* **2003,** *75*(8), 1887–1894.
45. Shortt, D. W. Measurement of Narrow-Distribution Polydispersity Using Multiangle Light Scattering. *J. Chromatogr. A* **1994,** *686*(1), 11–20.
46. Zhigilei, L.V.; Garrison, B. J. Microscopic Mechanisms of Laser Ablation of Organic Solids in the Thermal and Stress Confinement Irradiation Regimes. *J. Appl. Phys.* **2000,** *88*(3), 1281–1298.
47. Freiser, B. S., Ed., *Organometallic Ion Chemistry (Understanding Chemical Reactivity, Vol. 15*; Kluwer: Dordrecht, The Netherlands, 1996; p. 335.
48. Lehmann, E.; Knochenmuss, R.; Zenobi, R. Ionization Mechanisms in Matrix-Assisted Laser Desorption/Ionization Mass Spectrometry: Contribution of Preformed Ions. *Rapid Commun. Mass Spectrom.* **1997,** *11*(14), 1483–1492.
49. Rashidezadeh, H.; Guo, B. Investigation of Metal Attachment to Polystyrenes in Matrix-Assisted Laser Desorption Ionization. *J. Am. Soc. Mass Spectrom.* **1998,** *9*(7), 724–730.
50. Hanton, S. D.; Owens, K. G.; Chavez-Eng, C.; Hoberg, A.-M.; Derrick, P. J. Updating Evidence for Cationization of Polymers in the Gas Phase During Matrix-Assisted Laser Desorption/Ionization. *Eur. J. Mass Spectrom.* **2005,** *11*(1), 23–29.
51. Walker, K. L.; Kahr, M. S.; Wilkins, C. L.; Xu, Z.; Moore, J. S. Analysis of Hydrocarbon Dendrimers by Laser Desorption Time-of-Flight and Fourier Transform Mass Spectrometry. *J. Am. Soc. Mass Spectrom.* **1994,** *5*(8), 731–739.
52. Grosberg, A. Yu.; Khokhlov, A. R. *Statistical Physics of Macromolecules*; AIP: New York, 1994; p. 350.
53. Mandelkern, L. *Crystallization of Polymers, Vol I. Equilibrium Concepts*, 2nd ed.; Cambridge University Press, Cambridge, UK: 2002; pp 550.
54. Kurikawa, T.; Takeda, H.; Hirano, M.; Judai, K.; Arita, T.; Nagao, S.; Nakajima, A.; Kaya, K. Electronic Properties of Organometallic Metal-Benzene Complexes [*Mn(benzene)m (M = Sc-Cu)*]. *Organometallics* **1999,** *18*(8), 1430–1438.
55. Le Bozec, H.; Touchard, D.; Dixneuf, P. H. Organometallic Chemistry of Arene Ruthenium and Osmium Complexes. *Adv. Organomet. Chem.* **1989,** *29,* 163–247.
56. Ries, M. D. Enhanced Polyethylene Implants: Have We Been There Before? *Instructional course lectures* **2005,** *54,* 189–192.
57. Montaudo, G.; Puglisi, C.; Samperi, F.; Carroccio, S. MALDI-TOF Investigation of Polymer Degradation: Pyrolysis of Poly(Bisphenol A Carbonate). *Proceedings of the, 219th ACS National Meeting, (Book of Abstracts)*; San Francisco, CA, March, 2000; p POLY-429.